

ОБЪЕДИНЕННЫЙ  
ИНСТИТУТ  
ЯДЕРНЫХ  
ИССЛЕДОВАНИЙ  
ДУБНА

E7-86-732

W. Augustyniak, C. Borcea, M. Lewitowicz,  
Nguyen Hoai Chau, Yu. E. Penionzhkevich,  
V. G. Sandukovski, M. Sowiński\*, S. Chojnacki

EXPERIMENTAL STUDY  
OF  $\alpha$ -FISSION FRAGMENT CORRELATIONS  
IN THE  $^{232}\text{Th}(^{12}\text{C}, \alpha f)$  REACTION

Submitted to "Journal of Physics G:  
Nuclear Physics"

\* National Atomic Energy Agency, Warsaw, Poland

1986

## I. Introduction

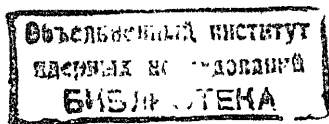
One of the most interesting processes involved in heavy ion interactions at about 10 MeV/nucleon is fast light particle emission. This process, despite many theoretical efforts made, is not yet completely understood <sup>/1,2/</sup>. Nevertheless, it may be used to "prepare" different nuclei and study their properties. Heavy ion reactions in which fast light particles are emitted may be used to produce "cold" heavy nuclei and subsequently to study their fission. The fast particle energy is directly related to the excitation energy of the residual nucleus in analogy with the situation observed in the fission studies performed with light particle induced transfer reactions <sup>/1/</sup>.

The purpose of the present work was to study the influence of the angular momentum brought into the system by the heavy projectile on the fission channel as well as to clarify the role of the excitation energy of the fissioning nucleus. With this aim, the mass and total kinetic energy (TKE) distributions were measured in and without coincidence with the  $\alpha$  particles emitted in the reaction  $^{12}\text{C}(85 \text{ MeV}) + ^{232}\text{Th}$ . Correlation measurements offered a possibility of defining the reaction exit channel and of establishing the mechanism of  $\alpha$  particle emission. The main characteristics of fission of the heavy nuclei produced in this reaction were studied in detail in reactions induced by neutrons and light charged particles <sup>/3,4/</sup>. The choice of the reaction was made so that the excitation energy of the compound nucleus  $^{244}\text{Cm}$  was not very high ( $E^* \sim 58 \text{ MeV}$ ) and also its introduced angular momentum had relatively low values ( $l_{\text{max}} \sim 37 \hbar$ ).

## II. Experimental technique

The present measurements were performed using 85 MeV  $^{12}\text{C}$  ion beams from the Laboratory of Nuclear Reactions cyclotron U200. The target was a self-supported metallic  $^{232}\text{Th}$  foil ( $1 \text{ mg/cm}^2$ ) placed at an angle of 40 degrees with respect to the beam axis.

Coincident fission fragments were detected with a pair of position-sensitive semiconductor detectors (PSD) placed at  $\pm 80^\circ$  symmetrically on both sides of the beam, each subtending an angle of  $80^\circ$  in the reaction plane. Charged particles were detected with three  $\Delta E-E$  telescopes each consisting of  $60 \mu\text{m}$  and 2 mm Si detectors. Two of them were placed at angles of  $20^\circ$  and  $140^\circ$  in the reaction plane. The third was located in the vertical plane containing the beam axis at  $145^\circ$  (Fig. 1). The inclusive spectra of  $^4\text{He}$  were measured by rotating one of the telescopes from  $20^\circ$  to  $160^\circ$  in steps of  $10^\circ$ . Due to the aluminium absorber of  $120 \mu\text{m}$  thickness located in front of the  $\Delta E$  detector at forward angles, the minimum detectable alpha energy was 20 MeV. At backward angles the experimental alpha energy threshold was 8 MeV. Beam intensity was monitored by a Faraday cup and by a monitor detector placed at  $10^\circ$ . The alpha particle telescopes were calibrated with a  $^{226}\text{Ra}$  alpha source and with a precision



pulsar. The energy calibration of the two PSD was made by measuring the energy spectra of fission fragments from the  $^4\text{He}$  (34 MeV) +  $^{232}\text{Th}$  reaction and using the Schmitt /5/ calibration procedure. The mass distributions were obtained on the following assumptions: a) The sum of the masses of primary fission fragments is equal to that of the target and the projectile. b) The sum of the fragment momentum components perpendicular to the beam axis is equal to zero. We estimated the accuracy of the fission fragment mass measurements to be  $\sim 5\%$ .

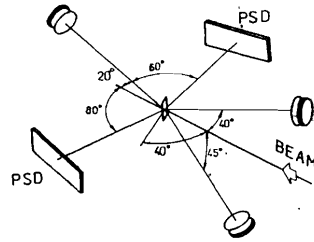


Fig. 1. The experimental set-up.

For the position calibration of the PSD two wires were placed in front of each detector. Due to uncertainties in the beam position on the target the fission fragment folding angle was measured with an accuracy of  $\sim 2^\circ$ . For the inclusive measurements of the light charged-particle spectra reactions of the beam with light element impurities of the target play an important role /6/. In order to subtract this effect from the experimental results we measured for each angle the alpha spectra for a standard carbon target and for the Th target at two bombarding energies: 85 MeV and 53 MeV. We assumed that at the latter energy, which is 13 MeV lower than the intrinsic Coulomb barrier for the  $^{12}\text{C} + ^{232}\text{Th}$  reaction, carbon ions interact only with light elements (C, O, N). Then, at this energy after the normalization using the Faraday cup, the ratio between the  $\alpha$  particles yields from the Th target and from a pure C target gives straightforwardly the amount of C impurities in the Th target. Subsequently, the  $\alpha$  spectra obtained for the C target were multiplied by the ratio described above and then subtracted from the  $\alpha$  spectra obtained for the Th target at each angle. According to our estimates, about 20% of alpha particles were emitted from impurities at  $20^\circ$ . Figure 2 shows an example of the alpha spectra used for such corrections at  $20^\circ$  and  $120^\circ$ ; the contribution from light element impurities at backward angles is very small.

The coincidences between fission fragments and alpha particles and inclusive alpha energy spectra were recorded event by event on magnetic disc and subsequently analysed off-line. Some details of the experimental setup are presented in /7/.

### III. Results and discussion

#### 1. $\alpha$ -particle spectra

The measured inclusive spectra of  $\alpha$  particles emitted at several angles between  $20^\circ$  and  $160^\circ$  (lab) are shown in fig. 3. The most prominent feature is the two-component structure of these spectra which shows up at angles greater than  $50^\circ$ ; one may distinguish a low-energy and high-energy component. At smaller angles the two components merge together. The high-energy component gradually increases in

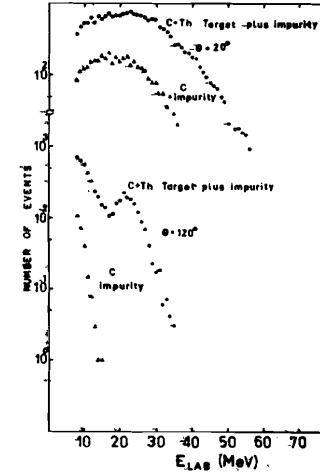


Fig. 2. Contribution to the inclusive  $\alpha$  energy spectra from the light element impurities in target material, determined as described in sect. II.

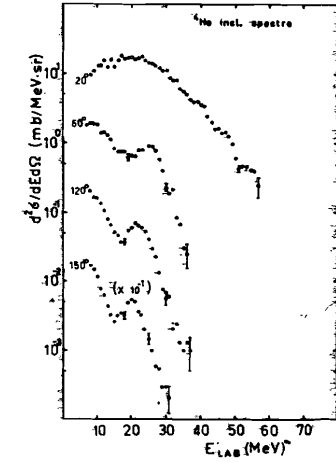


Fig. 3. Inclusive  $\alpha$  particle spectra measured for the reaction  $^{12}\text{C}$  (85 MeV) +  $^{232}\text{Th}$ .

intensity and its maximum shifts toward higher energies close to the Coulomb barrier in the exit channel (24 MeV in the lab.system), which in the given case almost coincide with the energy corresponding to the beam velocity (28 MeV). The observed  $\alpha$  particles may originate from a number of sources and as a result of different reaction mechanisms /1,2,12,13/, e.g. evaporation from the compound nucleus, evaporation from the excited fission fragments; ternary fission, projectile break-up or break-up fusion,  $\alpha$  activity of the different nuclei produced in fusion of the projectile (or part of it) with the target followed by neutron or charged-particle evaporation, preequilibrium emission, and others. It is rather difficult to evaluate how much each of these mechanisms contributes to the inclusive spectra of the  $\alpha$  particles. In the present work we tried to estimate only the most significant of them. The energies of  $\alpha$ 's coming from different activities are less than  $\sim 10$  MeV. Also, the  $\alpha$ 's evaporated from the fission fragments have most probable energies in the frame linked to the fragment equal to the exit Coulomb barriers. In the CM system, due to the random orientation of the fragments, these  $\alpha$ 's have the most significant yield at energies almost twice lower than the energies of the  $\alpha$ 's evaporated from the compound nucleus. In the lab. system this will amount to no more than 15 MeV. These two processes make the main contribution to the low-energy part of the inclusive spectra, especially at backward angles. For the  $E_{\alpha} > 15$  MeV part of the spectra, the main contribution is brought in by evaporation from the compound nucleus, by

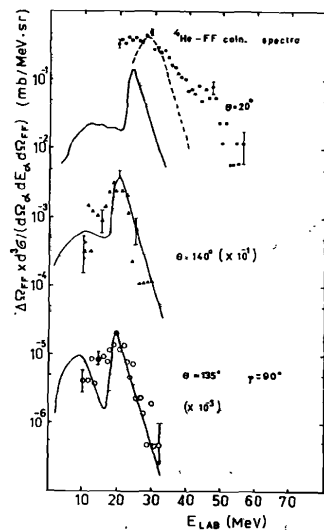
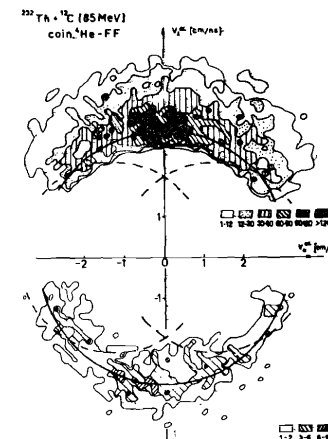


Fig. 4. The  $\alpha$ -particle spectra measured in coincidence with fission fragments. The full line shows the result of a Monte-Carlo simulation calculation for the particles evaporated by the compound nucleus and by the fission fragments. The dashed line represents the result of a break-up calculation, as described in /9/.

precompound emission and projectile break-up. It is known that all these mechanisms give rather broad distributions in energy that overlap with each other. In order to further elucidate the different contributions, the coincidences of  $\alpha$  particles with fission fragments were measured. The  $\alpha$ 's were recorded at  $20^\circ$  and  $140^\circ$  in the reaction plane and at  $45^\circ$  in a plane containing the beam and perpendicular to the reaction plane (defined as the plane in which the fission fragment detectors and the beam lay, see fig. 1). The measured coincident spectra are shown in fig. 4. One can see that the shape of the spectrum at  $20^\circ$  is quite similar to its inclusive analog. For the backward angles, the difference between the inclusive and coincident spectra is clearly seen for energies  $< 15$  MeV and may be explained by the absence in the coincident spectrum of the contributions from the  $\alpha$  activities induced in the target. The coincidence data were also used to build the contour diagram of differential cross section  $G_v = \Delta\Omega_f d^3G / (dV_\alpha d\Omega_\alpha d\Omega_f)$  (fig. 5). In this diagram the coordinates are given by the projections of  $\alpha$  velocity in the CM system on the direction of flight of the heavy fragment (x axis) and perpendicular to it, respectively (y axis). The full and dashed lines represent the most probable velocity values of  $\alpha$  particles evaporated from the compound nucleus and from the fission fragments, respectively. For the backward hemisphere, the  $\alpha$  emission is well accounted for by evaporation from the compound nucleus and from fission fragments. At forward angles the velocity distribution shifts toward higher values indicating the presence of the nonevaporation mechanisms. A Monte-Carlo simulation calculation was performed using the program ELPHIC /8/. In this calculation evaporation from the compound nucleus and from the fission fragments was considered. The relative intensity of these two

Fig. 5. Two-dimensional plot of the cross section  $G_v$  (see the text).  $v_{||}^\alpha$  and  $v_{\perp}^\alpha$  are the projections of the particle velocity on the directions of emission of the heavy fragment in the CM system and perpendicular to it. The scale for  $G_v$  is in arbitrary units. The lines are explained in the text.



components and the overall normalization were chosen so as to reproduce the spectrum at  $140^\circ$ . Then, with these parameters unchanged, the calculations were repeated for other angles. The results are shown in fig. 4 by the full line. One can see that the evaporation process makes only a rather small contribution to  $\alpha$  emission at  $20^\circ$ ; the rest of it should be ascribed to some other processes like projectile break-up and/or preequilibrium emission. Due to the  $\alpha$  cluster structure of the  $^{12}\text{C}$  projectile it is justifiable to assume that an important role in the forward  $\alpha$  particle emission is played by the projectile break-up followed or not (depending on the impact parameter) by the fusion of the projectile residue with the target nucleus. Following a procedure /9/ based on the Serber break-up model /10/ one may calculate the shape of the spectra of  $\alpha$  particles coming from the break-up fusion process. The results of the calculations are shown in fig. 4 (the dashed line), after being normalised to the experimental data in the maximum of the spectra. Obviously, such a mechanism cannot explain the high-energy part of the measured spectra. The break-up of the  $^{12}\text{C}$  projectile into three  $\alpha$  particles (without fusion) gives wider spectral shapes but it is difficult to estimate the contribution from such a process to the measured spectra.

To sum up the following conclusions can be drawn:

(1) The inclusive  $\alpha$  spectra have a two-component structure: one may distinguish a low-energy ( $E_\alpha < 15$  MeV) and a high-energy ( $E_\alpha > 15$  MeV) component. At small angles the two components are not distinguished from one another.

(2) Evaporation from the composite system and from the fission fragments can account for the spectra measured at backward angles but this process makes a rather small contribution to the forward  $\alpha$  particle emission.

## 2. Fission fragment measurements

### a. Linear momentum transfer (LMT).

LMT analysis offers the possibility to determine the dominant reaction channels contributing to the measured  $(f_1, f_2)$  correlations. LMT distributions studied in the present reaction are well described by Gaussian functions centered on the most probable value:  $\overline{LMT}$ . The FWHM amounts to about 30% of the  $\overline{LMT}$  value. The error of LMT determination is  $\sim 5\%$  due to the errors of angle and energy measurements for the fission fragments.

For the  $\alpha$ -fission fragment coincidences the LMT is defined as the sum  $P_{\alpha} + P_{f_1} + P_{f_2}$ , where  $P$  is the momentum projection on the beam axis and the subscripts stand for  $\alpha$  particle and fission fragments, respectively. The  $\overline{LMT}$  value for the correlation measurements in which  $\alpha$  particles were recorded at  $20^\circ$  amounts to 100% of the full momentum transfer (equal to the beam momentum,  $P_{beam}$ ). If we exclude the  $\alpha$  momentum from the above sum, then the distribution of the  $P_{f_1} + P_{f_2}$  has a mean value that is only 65% of the full momentum transfer or, in other words, only 2/3 of the beam momentum. This, together with the observation that at forward angles evaporation processes give a small contribution, indicates that in most of the cases the  $^{12}\text{C}$  projectile breaks up into an  $\alpha$  particle that flies away and a heavy part that fuses with the target nucleus.

For the correlation measurements in which  $\alpha$ 's were recorded at  $140^\circ$  the distribution of the sum  $P_{f_1} + P_{f_2}$  has its most probable value (centroid) at 115% of  $P_{beam}$ ; when  $P_{\alpha}$  is added,  $\overline{LMT}$  reaches a value of 100% of  $P_{beam}$ . The  $\overline{LMT}$  distribution for the fragment-fragment correlation measurement is centered around a value which constitutes 93% of  $P_{beam}$ . This high value is a proof of the dominant role of compound nucleus formation in the given reaction. According to the analysis performed in <sup>13/</sup> for similar reactions, one may presume that the difference of up to 100% is due to light particle emission prior to fission.

### b. Fission-fragment mass distributions.

One of the most significant features of the fission channel is the fragment mass distribution. For the case studied these distributions are shown in fig. 6 for  $(f_1, f_2)$  and  $(\alpha f_1, f_2)$  correlations. In both cases one can observe bell-shaped distributions without any evident two-humped structure. As it was shown in the previous section, these distributions correspond mainly to the fission of the compound nucleus  $^{244}\text{Cm}$  (the  $f_1, f_2$  case) or to the fission of  $^{240}\text{Pu}$  (the  $\alpha f_1, f_2$  case). For the  $(f_1, f_2)$  correlations, on the basis of peak-to-valley systematics as a function of the excitation energy of the fissioning nucleus produced by neutron-induced reactions <sup>13/</sup> one may expect that any two-humped structure should disappear as the excitation energy of the compound nucleus is equal to 58 MeV. In the case of  $(\alpha f_1, f_2)$  correlations, however, the systematics given in <sup>14/</sup> for reactions induced by protons and  $\alpha$  particles indicate a peak-to-valley ratio for  $^{240}\text{Pu}$  equal to 1.3 (or 1.5 according to <sup>13/</sup>). These values are obtained for a mean excitation energy

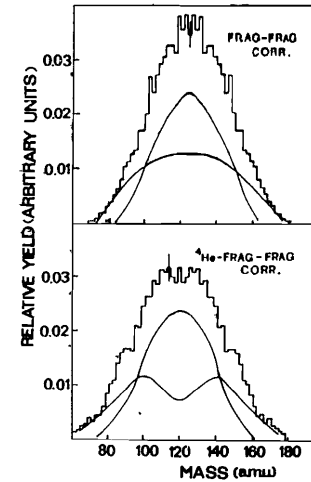


Fig. 6. Fission-fragment mass distributions for the reaction  $^{12}\text{C}(85 \text{ MeV}) + ^{232}\text{Th}$ . (a) the  $(f_1, f_2)$  correlations; (b) the  $(\alpha f_1, f_2)$  correlations. Dashed lines are fits to the data considering contributions from the two fission modes: asymmetric and symmetric ones. The fit parameters are given in Table 1.

of  $^{240}\text{Pu}$  equal to 37 MeV which corresponds to the most probable  $\alpha$  particle emission energy of 25 MeV in the lab.system.

If the measured mass distributions are the combined result of two fission modes, namely the symmetric and asymmetric ones, then the obtained result is an indication that in the present case the symmetric mode plays a more important role than in the case of reactions induced by light particles (leading to the formation of the same fissioning system).

A strong dependence of the shape of the mass distributions on the total kinetic energy (TKE) was observed (see fig. 7). For  $\text{TKE}_{lab} < 160 \text{ MeV}$  the mass distributions

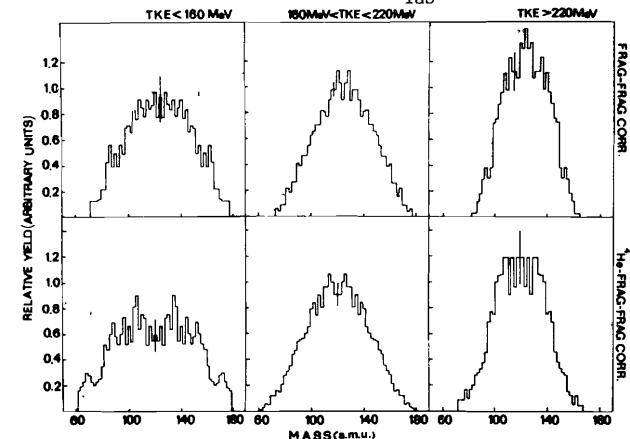


Fig. 7. Fission fragment mass distributions for three different windows on TKE. First row - the  $(f_1, f_2)$  correlations; second row - the  $(\alpha f_1, f_2)$  correlations.

look fully asymmetric (with peaks lying near masses of 100 and 140) while for  $TKE_{lab} > 220$  MeV they look quite symmetric. For intermediate  $TKE$  values the mass distributions have wide bell-shaped forms. Such a dependence of the shape of the mass distribution on  $TKE$  was observed for fission of  $^{240}\text{Pu}$  ( $\alpha f_1 f_2$  correlations) as well as for fission of  $^{244}\text{Cm}$  ( $f_1 f_2$  correlations). This result offers the possibility to divide the mass distribution into their symmetric and asymmetric components. The asymmetric mass distribution obtained for  $TKE_{lab} < 160$  MeV was fitted by two gaussians while the mass distribution obtained for  $TKE_{lab} > 220$  MeV was fitted only with one gaussian. Then, keeping the obtained shapes unchanged, their weights were chosen in order to reproduce the total mass distribution. The results of such a decomposition are shown in fig. 6 (full lines) and given in Table 1. The obtained ratios of the symmetric yield to the total yield  $Y_{sym}/Y_{tot}$  were compared with the results of <sup>/15/</sup> in which the fission of  $^{239}\text{Pu}$  was studied at an excitation energy of 36 MeV. In <sup>/15/</sup> the  $^{239}\text{Pu}$  nucleus was produced by bombarding  $^{235}\text{U}$  and  $^{236}\text{U}$  target with  $^4\text{He}$  and  $^3\text{He}$  ions, respectively. The mean angular momentum of the compound nucleus in these two cases was 16  $\hbar$  and 8  $\hbar$ , respectively. Fitting the mass distribution given in <sup>/15/</sup> by three gaussians allows the evaluation of the contributions from the symmetric and asymmetric fission modes. The three gaussians were centered on masses 100, 120 and 140 according to the prescriptions taken from <sup>/16/</sup>. The obtained ratios  $Y_{sym}/Y_{tot}$  and the fit parameters are given in Table 1. They show the increasing role of the symmetric fission mode as the angular momentum of the fissioning nucleus increases.

Table 1.

Parameters and results of the three-Gaussian fits of the experimental mass distributions

Fissioning compound nucleus (reaction)	$E^*$ /MeV/	$\langle l \rangle$ / $\hbar$ /	Asym. fission				Sym. fission		$Y_{sym}/Y_{tot}$
			$\bar{M}_L$	$\sigma_L$	$\bar{M}_H$	$\sigma_H$	$\bar{M}$	$\sigma$	
$^{244}\text{Cm}$ (b) ( $^{12}\text{C} + ^{232}\text{Th} \rightarrow \text{ff}$ )	58	25							0.58 $\pm$ 0.05
$^{240}\text{Pu}$ (b) ( $^{12}\text{C} + ^{232}\text{Th} \rightarrow \text{ff} + \alpha$ )	37	32							0.55 $\pm$ 0.05
$^{239}\text{Pu}$ (a) ( $^4\text{He} + ^{235}\text{U}$ )	35.9	16.4	100	8.5	139	8.5	120	12	0.42 $\pm$ 0.02
$^{239}\text{Pu}$ (a) ( $^3\text{He} + ^{236}\text{U}$ )	35.9	7.6	101	8.5	139	8.5	120	12	0.26 $\pm$ 0.02

a - experimental data taken from Cuninghame and Goodall <sup>/15/</sup>

b -  $Y_{sym}/Y_{tot}$  obtained in the present paper (see the text)

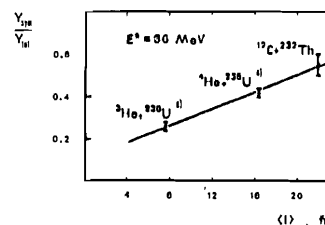


Fig. 8. Dependence of the symmetric fission to the total fission yield ratio on the mean angular momentum of the fissioning nucleus. Points a - are taken from the results of Cuninghame and Goodall <sup>/15/</sup>.

For the present reaction, the mean values of the angular momentum of the fissioning nuclei were obtained as follows: for  $^{244}\text{Cm}$   $\langle l \rangle$  was taken as  $2/3 l_{max}$ ; the value obtained was  $\langle l \rangle = 25 \hbar$ . For  $^{240}\text{Pu}$  we had to include the mean angular momentum carried away by the  $\alpha$  particles recorded at  $20^\circ$  and having the most probable energy of 25 MeV. The resulting value was  $\langle l \rangle = 22 \hbar$ . In fact, the latter value is probably underestimated as the break-up fusion reaction which in the given case plays an important role (see the previous reaction) is a peripheral reaction.

The dependence of the ratio  $Y_{sym}/Y_{tot}$  on  $\langle l \rangle$  obtained for  $^{239}\text{Pu}$  studied in <sup>/15/</sup> and for  $^{240}\text{Pu}$  studied in the present work at close excitation energies appears to be linear in the first approximation (see Table 1 and fig. 8).

As it was shown in <sup>/15/</sup> for the reactions induced by  $^3\text{He}$  and  $^4\text{He}$  in about 30% of the cases second or third chance fission occurs, after the emission of one or more particles. Obviously, particle emission leads to a decrease in the excitation energy of the fissioning nucleus and, correspondingly, to an enhancement of the asymmetric fission mode as at lower excitation energies shell effects play a more important role. In the present experiment, the enhancement of the symmetric fission mode indicates the increased fissility to the detriment of the particle emission probability. A possible interpretation of such a result is the following: with an increase in the projectile mass, the angular momentum brought into the system also increases. On the other hand, massive projectiles are capable of producing shape oscillations of large amplitude which, together with the high values of the angular momentum, may lead to an enhanced fissility. Moreover, one may presume that for heavy projectiles the transition from the saddle point to scission is so fast that shell effects fail to manifest themselves entirely. Besides, for larger  $\langle l \rangle$  values, the probability for symmetric fission grows due to the increased values of the centrifugal forces. Such a representation reminds of the fast fission process that shows up at higher bombarding energies and for larger projectile masses.

For the case of ( $\alpha f_1 f_2$ ) correlations, the dependence of the mass distribution on the particle energy was also studied. For this purpose, the spectra were divided into a low energy ( $E_\alpha < 35$  MeV,  $\bar{E}_\alpha = 25$  MeV) and a high energy part ( $E_\alpha > 35$  MeV,  $\bar{E}_\alpha = 40$  MeV). The corresponding mass distributions do not show significant changes of their shapes.

Such a result can be explained as follows. The low energy part of the spectra contains most of the cross section and the dominant process in the break-up fusion (see sect. III2a). The high energy part, having a much smaller cross section contains contributions both from break-up fusion and from the tree-body break-up of  $^{12}\text{C}$ . The three-body break-up ( $^{12}\text{C} + ^{232}\text{Th} \rightarrow \alpha + \alpha + \alpha + ^{232}\text{Th}$ ) reaction has the Q value that is about 10 MeV higher than that of the break-up fusion reaction. If one assumes that in this energy interval the three-body break-up takes over the break-up fusion (as fig. 4 tends to suggest), then the extra energy due to the reaction Q value almost compensates for the increase in the mean  $\alpha$  energy. Thus, in fact the excitation energy of the fissioning nucleus is essentially the same for the two window settings on the  $\alpha$  particle energy. The main conclusions from the above analysis of the LMT and mass distributions are as follows:

- 1) The obtained LMT distributions show, in the case of  $(f_1 f_2)$  correlations, the dominance of  $^{244}\text{Cm}$  compound nucleus fission and the dominance of  $^{240}\text{Pu}$  fission in the case of  $(\alpha f_1 f_2)$  correlations.
- 2) The enhanced symmetric fission of  $^{240}\text{Pu}$ , as compared with that observed in reactions induced by light ions, may be explained by enhanced fissility resulting from the angular momentum brought into the system and from the massivity of the projectile.
- 3) The observed shape of the mass distributions does not depend significantly on the emitted  $\alpha$  particle energy. This seems to be a combined effect of the projectile  $\alpha$  cluster structure and of the Q values of different contributing exit channels.

#### Acknowledgments

The authors are indebted to Prof. Yu.Is.Oganessian for his permanent interest in the present work and to Dr. B.I.Pustylnik for stimulating discussions.

#### References

1. Penionzhkevich Yu.E., Gierlik E., Kamanin V.V., Borcea C. Phys.Elem.Part.and Atomic Nuclei (Sov) 17 (1986) 165 and references therein.
2. Betak E., Toneev V.D. Phys.Elem.Part.and Atomic Nuclei (Sov) 12 (1981) 1432 and references therein.
3. Von Gunten H.R. Actinides Rev. 1 (1969) 275.
4. Wagemans C.M.C., Wegener-Penning G., Weigmann H., Barthelemy R. Proc. of Symp. Phys. and Chem. of Fission, Jülich, 14-18 May 1979, vol.II, p.143.
5. Schmitt H.W., Kicker W.E., Williams C.W. Phys. Rev. 137B (1965) 837.
6. Vaz L.C., Logan D., Duek E., Alexander J.M., Rivet M.F., Zisman M.S., Kaplan M., Ball J.W. Z.Phys. A315 (1984) 169.
7. Sowiński M., Lewitowicz M., Kupczak R., Jankowski A., Skobelev N.K., Chojnacki S. Z.Phys. 323 (1986) 87.
8. Lewitowicz M. Preprint JINR, P11-84-284, Dubna, 1984.
9. Magda M.T., Pop A., Sandulescu A. Journal of Nucl. Phys. (Sov) 43 (1986) 1176.

10. Serber D. Phys. Rev. 72 (1947) 1008.
11. Aves T.C., Poggi G., Saini S., Colbko C.K., Legrain R., Westfall G.P. Phys. Lett. 103B (1981) 417.
12. Aves T.C., Poggi C., Gelbko C.K., Back B.B., Ciagola B.G., Breuer H., Viola V.E. J.Phys.Rev. C24 (1981) 89 and references therein.
13. Duek E., Kowalski L., Rajngopalan M., Alexander J.M., Debiak T.W., Logan D., Kaplan M., Zisman M., Lo Beyoc Y. Z.Phys. A 307 (1982) 221.
14. Dccowski P., Moroch H.P., Zomzo L., Rogge M., Turek R. Annual Report, Nucl.Phys. Laboratory, Instituto of Experim. Physics, Warsaw University, 1984, p.30.
15. Cuninghame J.G., Goodall J.A.B. Journ. Phys.G: Nucl.Phys. 1 (1975) 250.
16. Thierens H., DoClercq A., Jacobs E., DeFrenne D., D'hondt P., De Gelder P., Deruytter A.J. Phys. Rev. C 23 (1981) 2104.

Received by Publishing Department  
on November 11, 1986.

## SUBJECT CATEGORIES OF THE JINR PUBLICATIONS

Index	Subject
1.	High energy experimental physics
2.	High energy theoretical physics
3.	Low energy experimental physics
4.	Low energy theoretical physics
5.	Mathematics
6.	Nuclear spectroscopy and radiochemistry
7.	Heavy ion physics
8.	Cryogenics
9.	Accelerators
10.	Automatization of data processing
11.	Computing mathematics and technique
12.	Chemistry
13.	Experimental techniques and methods
14.	Solid state physics. Liquids
15.	Experimental physics of nuclear reactions at low energies
16.	Health physics. Shieldings
17.	Theory of condensed matter
18.	Applied researches
19.	Biophysics

Аугустыняк В. и др.

E7-86-732

Экспериментальное исследование корреляций осколков деления с  $\alpha$ -частицами в реакции  $^{232}\text{Th}(^{12}\text{C}, \alpha f)$

Проведены измерения инклюзивных и корреляционных спектров  $\alpha$ -частиц и осколков деления в реакции  $^{232}\text{Th} + ^{12}\text{C}$  (85 МэВ) с целью выделения разных механизмов их эмиссии. Для задних углов эмиссию  $\alpha$ -частиц можно объяснить испарительными процессами. Для передних углов доминирующим является процесс развал-слияние. Получены также массовые распределения осколков деления составных ядер  $^{244}\text{Cm}$  ( $E^* = 58$  МэВ,  $ff$ -совпадения) и  $^{240}\text{Pu}$  ( $E^* = 37$  МэВ,  $ff_{\alpha}$ -совпадения). В случае ядра  $^{240}\text{Pu}$  форма массового распределения осколков отличается от полученной в реакции с легкими ионами, что свидетельствует о сильном влиянии входного канала. Была также изучена зависимость формы массового распределения осколков от  $\alpha$ -частиц. Отсутствие зависимости массового распределения от энергии испускаемой  $\alpha$ -частицы объясняется кластерной структурой ядра-снаряда и разницей в величинах для различных каналов реакций.

Работа выполнена в Лаборатории ядерных реакций ОИЯИ.

Препринт Объединенного института ядерных исследований. Дубна 1986

Augustyniak W. et al.

E7-86-732

Experimental Study of  $\alpha$ -Fission Fragment Correlations in the  $^{232}\text{Th}(^{12}\text{C}, \alpha f)$  Reaction

Inclusive and coincident spectra of alpha particles and fission fragments were measured for the  $^{232}\text{Th} + ^{12}\text{C}$  (85 MeV) reaction, with the aim of separating different mechanism contributions. At backward angles  $\alpha$  emission can be accounted for by the evaporation processes. At forward angles the most important contribution is given by the break-up fusion process. Mass distributions for compound nuclei  $^{244}\text{Cm}$  ( $E^* = 58$  MeV,  $ff$  coincidences), and  $^{240}\text{Pu}$  ( $E^* = 37$  MeV,  $ff_{\alpha}$  coincidences) were obtained. In the case of  $^{240}\text{Pu}$  mass distribution has a shape different from those obtained in light ion reactions at the same excitation energy indicating the strong influence of the entrance channel. The dependence of the mass distribution shape on the  $\alpha$ -particle energy is also examined. The weak dependence of this shape on the  $\alpha$  particle energy seems to be a combined effect of the projectile a cluster structure and of the Q values of different contributing exit channels.

The investigation has been performed at the Laboratory of Nuclear Reactions, JINR.

Preprint of the Joint Institute for Nuclear Research. Dubna 1986